INSTABILITY INDUCING POTENTIAL OF NEAR FAULT GROUND MOTIONS

Dionisio Bernal[1], Arash Nasseri[2] and Yalcin Bulut[2]

[1]Civil and Environmental Engineering Department, Center for Digital Signal Processing, Northeastern University, Boston, MA.
[2] Graduate Student, Northeastern University, Boston, MA,

Abstract

Gravity imposes a lower bound on the strength needed for stable response. Collapse spectra are plots of this strength vs. period for constant values of a parameter that characterizes gravity. The paper contains formulas for collapse spectral ordinates for near fault conditions and shows that the collapse mechanism in buildings is not statistically dependent on whether the excitation is near fault or far field. Safety against instability can be predicted using the provided expressions and results from a pushover analysis. The near fault condition is not found to be a critical consideration from an instability perspective.

Introduction

Dynamic instability is a phenomenon whereby the seismic response of a structure changes from vibration to unbounded drift in a single direction. Since the consequence of dynamic instability is complete collapse, characterization of this limit state is of paramount importance for the formulation of performance based seismic design guidelines. The salient feature of the instability phenomenon is the fact that it is abrupt. Indeed, as shown by Husid (1967), Jennings and Husid (1968), Takizawa and Jennings (1980) and Bernal (1990) for simple systems, and by Bernal (1992a, 1992b, 1998) using models of multistory structures, the influence of gravity on inelastic seismic response is generally small except for a small range of values where the strength of the system is near a threshold bellow which the response grows without bound. The situation is exemplified in fig.1 which depicts the maximum displacement at the first level of a model of a ten story building for increasing levels of a scaling factor that multiplies the ground motion amplitudes. The figure, which compares results from first order and second order nonlinear dynamic analyses shows that the maximum response is little affected by P-delta except in a restricted region near the strength for which instability occurs.

The behavior exemplified in fig.1 is typical and shows that the important issue in design is not assessing amplifications of the displacement response due to P-delta effects but establishing means to quantify the safety margin against the instability limit state. Note that the foregoing is not in harmony with the amplification approach that for many years has been used to consider P-delta effects in the analysis of buildings for wind, dead and live loads. Specifically, the amplification perspective is misleading because it suggests that the issue is one of "adjusting" the estimated response and this is not so. Plainly, since inertial loads during seismic excitation are not independent of structural characteristics the P-delta effect needs to be considered as a reduction in lateral stiffness, not as an added load. As noted, the important task from a practical

perspective is to characterize the instability limit in a way that is useful from the point of view of a designer that needs to ensure that safety against instability is adequate.

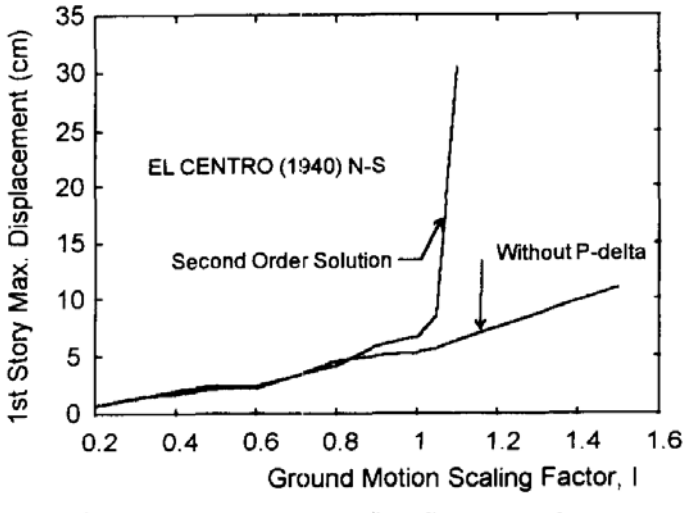

Fig.1 Maximum response at level#1 in a 10-story model of a steel frame

It is not difficult to see that experimental investigations to determine the collapse threshold or realistic structures subjected to earthquakes are impracticable. Virtually all the research in this area, therefore, is analytical. In this regard it is worth noting that formulation of high fidelity models for buildings that undergo large inelastic displacements is a very difficult task. For example, quantifying the participation of floor systems in providing lateral stiffness as a function of response history and amplitude is one of many items that can be listed as difficult to model accurately. An indication of the degree of simplification is the fact that while collapse takes places "downward", all our models for buildings predict it as large "lateral displacements".

Having accepted that analytical predictions of collapse are necessarily uncertain we must nonetheless move forward and make the best possible estimation given the constraints. While the "best" analytical prediction is in principle that obtained from a 3-D model that accounts for soil-structure interaction, non-structural element contributions, and which models the load-deformation relation of each structural element in as much detail as the state of knowledge allows, this model is generally impractical. In arriving at a practical solution one seeks, of course, to maximize reductions in the computational burden while adding the least possible uncertainty to the results. A brief summary of modeling related decisions made in this study is presented later in the paper and details can be found in the full report that appears in (Ref.1).

Assertions made in the previous paragraphs regarding instability are qualitative and independent of the specific characteristics of the ground motion. It has become increasingly clear in the past few decades, however, that records obtained in the close vicinity of the causative fault differ substantially from those in the far field and this has prompted concern on the adequacy of using design guidelines that have been validated using far field records in checking structures located close to known faults. The special feature of strong motion records obtained near faults is the fact that they often contain large velocity pulses of relatively long periods and/or large permanent displacements (Sommerville 1997, Rodriguez-Marek 2000). Prior to the project

reported on this paper research carried out on response to near fault motions had focused on characterizing the effect of near fault on linear and nonlinear effects, primarily on SDOF oscillators (MacRea,2001 and Mavroeidis,2004). The studies from these and other references produced consistent results and at present some modern codes (IBC-2004, FEMA356, ATC40) have incorporated near fault effects as modifiers of the elastic spectral ordinates (Table.1).

Table 1. Near fault modification factors for the acceleration (N_a) and velocity region (N_v) of the elastic response spectrum – as given in the IBC-2003 Code.

		N_a			N_v			
Type	Source	= 2 km	5 km	10km	= 2 km	5 km	10km	15km
A	M>7 SR≥5mm/yr	1.5	1.2	1.0	2.0	1.6	1.2	1.0
B	Not satisfying A or C	1.3	1.0	1.0	1.6	1.2	1.0	1.0
C	M=6.5 SR=2mm/yr	1.0	1.0	1.0	1.0	1.0	1.0	1.0

The question of whether or not structures located in the near fault require special treatment when it comes to the evaluation of the safety against instability is the basic question addressed in this study. For buildings in sites that are not too close to the seismic source the safety against this failure mode can be evaluated in terms of base-shear strength, shape of the controlling mechanism and the peak ground motion parameters and effective duration of the design motion (Bernal 1993, 1998). The research reported here shows that this framework can be used for near fault conditions also.

The paper is organized as follows. The first section following this introduction presents a summary of the existing methodology for characterizing instability, originally developed without regard for the frequency content of the records. The next section considers the development of statistical formulas for predicting collapse spectral ordinates for near fault conditions. Following the collapse spectra section the paper presents the results of a study on the instability of multistory structures. The results in this section are based on the examination of 3 structures varying from 6 to 20 stories in height. A summary and critical review of the findings concludes the paper.

Dynamic Instability Fundamentals

We adopt the definition that a structure subjected to a certain input is stable if small increases in the magnitude of the excitation result in small changes in the response. We begin by recalling that static stability can be ascertained by inspecting the eigenvalues [λ] of the effective tangent stiffness. In particular, since these eigenvalues represent generalized scalar stiffness values in the configuration of the associated eigenvectors [ϕ], static stability requires that all the terms in [λ] be positive. An equivalent more intuitive statement is that a structure is stable if the

change between any two equilibrium positions requires positive work from external forces. An obvious example of an unstable system is a ball on a slope. If one holds the ball in equilibrium by applying an external horizontal force and then allows it to move down the slope slowly to a new position the external work (not including gravity) is obviously negative. This example also shows that instability is associated with a specific direction, i.e., the ball roles down but not up. The parallel in a structural system is that the structure will deform "spontaneously" (with the help of gravity) in the direction of the eigenvector associated with the negative eigenvalue, not in other directions.

Configurations that are statically unstable can occur during dynamic response without resulting in collapse so the attainment of negative eigenvalues is a necessary but not a sufficient condition for dynamic instability. A mathematical discussion of how inertia provides the transient stabilizing forces that allow the system to "survive" configurations that are statically unstable is presented in Bernal (1998). Here, instead of repeating the mathematical treatment we clarify the basic behavior using a simple physical analogy. Consider, as shown in fig.2, the situation wherein a disc (to keep the problem in 2D) rests on a line whose concavity fluctuates dynamically from upward to downward. The disk represents the structure; the condition with upward concavity the times when the structure is statically stable and downward concavity that when yielding is so extensive that the tangent stiffness is insufficient to provide static stability. It should be apparent at this point that incursions into the downward concavity do not necessarily imply that the disc is going to roll down the surface and fall off. Namely, the outcome will depend on how long an unstable condition persists. Although the analogy is not precise, since in the situation of fig.2 the disc tends to return to a unique equilibrium position and this is not true in the structure, this flaw does not invalidate the basic idea which is that statically unstable configurations are necessary but not sufficient for dynamic instability.

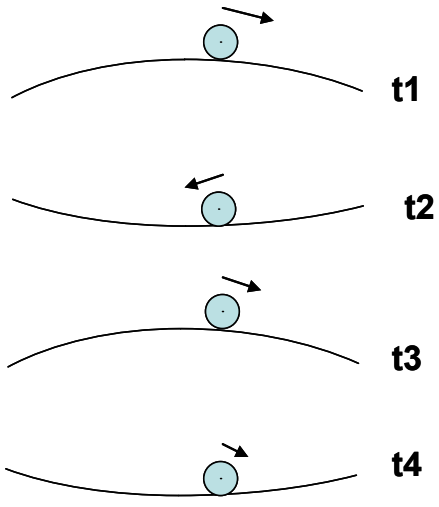

Fig.2 Analogy used to describe the ability of a structure to dynamically survive configurations that are statically unstable.

While it may appear at first glance that sufficient inelasticity to result in statically unstable configurations during earthquake response is unlikely, a closer look can dispel this first impression. The key point is that for negative eigenvalues to be attained there is no need for inelasticity to be such that the structure is rendered a mechanism. The point is illustrated in fig.3 which shows the variation of the fundamental buckling eigenvalue as a sequence of hinges progress up the structure. The structure in the figure is 6 stories high and the gravity load has been taken at a representative value, in particular, the buckling eigenvalue with no hinges is 10, which implies that the elastic buckling load is 10 times larger than the gravity loading condition considered. As the figure shows, if a wave of hinges that engages the beams of the lower 2 stories plus the column bases exists at any point the structural configuration is, from an instantaneous perspective, unstable.

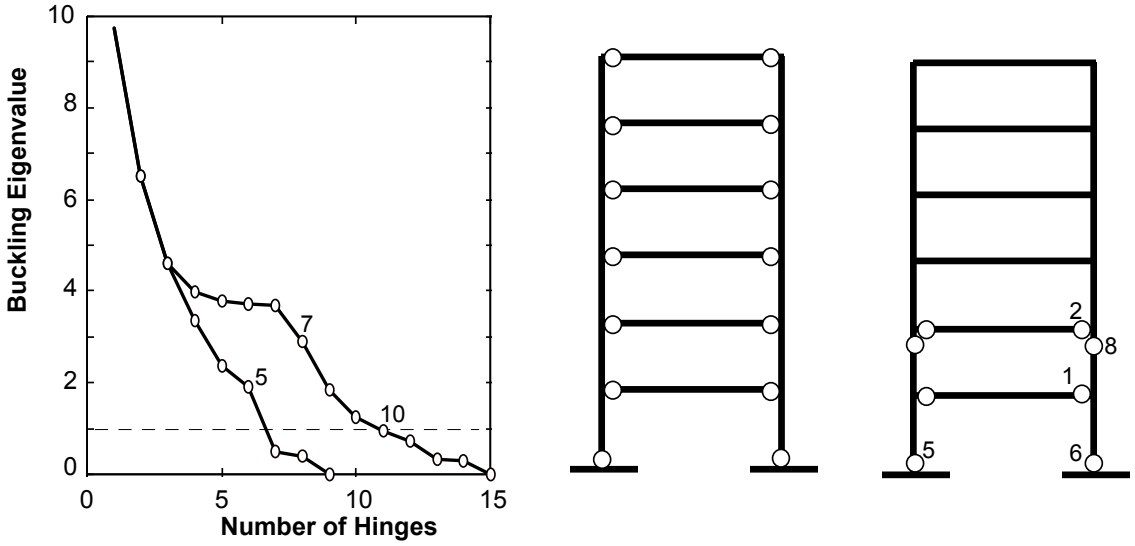

Fig.3 Buckling eigenvalue as a function of the distribution of plastic hinges

Characterizing the Effect of Gravity in the Load Deformation Behavior

The theory needed to formulate and analyze a full detailed model of a structure including nonlinearity and second order geometric effects is well established. Note that we do not imply here that it is easy or even possible to make a model that captures all the complexities of the real situation but simply that once the basic assumptions are made a material and geometrically nonlinear representation of a system can be formulated and analyzed. A direct check of the safety against instability by performing nonlinear dynamic analysis of a full model of each building is, however, impractical for routine application and for this reason simplified procedures compatible with the level of complexity of typical seismic provisions are necessary. Furthermore, it is in the reduced parameterization of a simplified method that the key parameters that affect behavior become clear and show which structural modifications have significant effect on the safety against instability and which do not.

The Stability Coefficient in a SDOF System

A parameter that has been widely used in simplified characterizations of second order gravity effects is the so called stability coefficient θ. The stability coefficient has been the subject of much discussion in the technical literature and is sometimes the source of confusion when sight is lost of the fact that there is no such thing as "the exact stability coefficient" for a multistory structure that responds nonlinearly, just like there is no such thing as "the ductility" at a given instant. The stability coefficient is non-dimensional parameter defined such that when multiplied by the first order elastic stiffness it gives the reduction in stiffness resulting from P-delta.

To clarify consider a rigid column supported at the base by a pin plus a nonlinear rotational spring. The column is assumed massless and weight is assumed concentrated at the tip as depicted in fig.4a. The load deformation relationship including the effect of the weight acting on the deformations can be easily computed and used to obtain the second order response. It is not difficult to see that the second order load deformation curve is obtained (in the simple situation of fig.4) by subtracting a constant slope from the first order curve. If we normalize the reduction in slope by the initial elastic slope one gets θ. In a MDOF system there is no unique load deformation curve and, even after one decides what function of the load to plot vs. what deformation the difference between the first order and second order curves is not, in general, a constant reduction in slope.

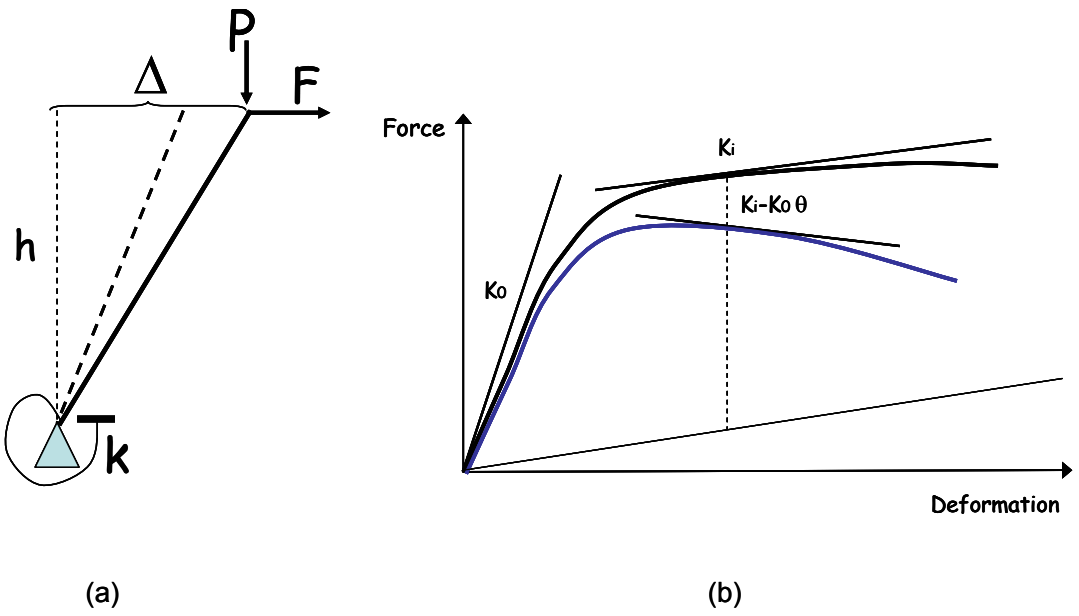

Fig.4 a) Rigid Column with rotational base spring b) First and second order load deformation curves.

The Stability Coefficient in a MDOF System

In a SDOF the value of θ is equal to the inverse of the elastic buckling eigenvalue. The buckling definition offers a tempting extension of the stability coefficient to the MDOF case but there is a need to be careful because the real question is not whether the definition is easily computed but whether the value is a good indicator of how gravity affects the potential for dynamic instability in buildings. To be explicit, if one tentatively accepts that there is a way to arrive at a SDOF model whose collapse occurs at the same ground motion intensity that produces instability in the real building, the question is whether a θ based on the elastic buckling eigenvalue is a good indicator of the difference between the first order and the second order load deformation of this SDOF system.

The answer, in general, is that the buckling based θ is not a good indicator and the reason has to do with the fact that in a MDOF system the reduction in slope of the load deformation due to P-delta depends on the predominant shape of the structure during the response and this shape, at large amplitudes can differ notably from the elastic buckling shape. Since in a first approximation the elastic buckling mode of a building is a straight line one concludes that the elastic buckling based θ should be reasonable when the governing mechanism is a global tilt.

Retaking the basic idea that θ is a way to specify how to pass from the first to the second order load deformation curve one has

Slope of 2^{nd} order load deformation = Slope of 1^{st} order - θ (Slope of first order at the origin)

from where one gets

$$\theta = \frac{\text{1st order slope} - \text{2nd order slope}}{\text{1st order at origin}} \tag{1}$$

MDOF to SDOF Reduction

The motivation for obtaining a reduction of the building to a SDOF system resides in the fact that instability can be characterized in terms of a few parameters in the SDOF case. In other words, if one can estimate when instability is imminent in a SDOF and has a procedure to reduce a multistory building to a SDOF then safety against instability in the building can be estimated without the need to perform nonlinear time history analysis of the full model. Reduction of a set of dynamic equilibrium equations to a single equation introduces approximation by necessity. The simplest approach to affect the reduction is by assuming a shape and solving for the amplitude. In this regard it should be noted that even in the simplest case of a linear system and a constant shape the solution is still not unique since there are various alternatives that arise from how the inevitable error is treated. To illustrate consider the equations of motion for earthquake input for a linear system which, neglecting damping can be written as

$$M\ddot{u} + Ku = -Mr\ddot{x}_g \tag{2}$$

To reduce the system to a SDOF we take

$$u \approx \phi Y \tag{3}$$

where ϕ is an assumed shape and Y is the amplitude. Substituting eq.3 into (2) gives

$$M\phi\ddot{Y} + K\phi Y = -Mr\ddot{x}_g + \varepsilon \tag{4}$$

where ε is a residual term that is needed because eq.3 is an approximation and eq.4 has been written as an equality. Since the left hand side of eq.4 has one unknown one can decide to satisfy the equality at a given DOF or, more generally, one can make any weighted sum of the terms in ε equal to zero and solve for the corresponding Y. Namely, with the weights listed in the vector φ one pre-multiplies by φ^T and taking $\varphi^T\varepsilon = 0$ gets the SDOF equation

$$\varphi^T M\phi\ddot{Y} + \varphi^T K\phi Y = -\varphi^T Mr\ddot{x}_g \tag{5}$$

Note that eq.5 depends not only on the assumed shape ϕ but also on the weights φ. The selection of $\varphi = \phi$ is, of course, common but is not forced by any compelling reason. Anyway, the point we set out to make is that even in the simplest case of linear behavior there are choices on how one arrives at the SDOF equation. In a study of instability the situation is much more complex because the assumption of a single dominant shape is not sufficiently general. Specifically, the shape of the structure when the response is not yet near collapse is governed by a shape that can usually be taken as the first mode but as the structure approaches failure the shape of the controlling mechanism dominates and this shape can vary notably from that of the first mode. A possibility that comes to mind is to perform a reduction using more than one shape but this is not a viable option since the characterization that is truly tractable is based on a SDOF model. The other possibility, initially examined by Pique (1976) and developed in detail for instability analysis by Bernal (1993) is to generalize the constraint in eq.3 as

$$u \approx Yf_Y \tag{6}$$

In other words, we assume a shape that is amplitude dependent. In Bernal (1993, 1998) and in the research reported here the amplitude dependent shape is taken as the sequence of deformed patterns that result from a pushover analysis using a mass proportional lateral load distribution. Description of the details of the SDOF reduction for the amplitude dependent shape is unnecessary for the present objectives and is thus skipped for brevity; the interested reader can find the details in the original references.

SDOF Reduction

1. Perform a first order pushover analysis with a load distribution that is proportional to the story weights (uniform in the case or regular buildings). From this analysis extract the

maximum base shear that the structure can withstand, V_u, and the parameters that define the shape of the final mechanism (see fig.5).

2. Calculate two stability coefficients. One that governs when the dominant shape is not far from the first mode, θ_0, and the other which accounts for the shape of the mechanism θ_m. The formulas are:

$$\theta_0 = \frac{g\tau}{\omega_0^2 h} \tag{7}$$

$$\theta_m = \Omega\theta_0 \tag{8}$$

with

$$\Omega = \frac{1 + 2N(1 - \frac{E}{h} - 0.5\frac{G}{h})}{\frac{G}{h}(1 + 2N(1 - \frac{E}{h} - 0.67\frac{G}{h}) + \frac{1}{3N}} \tag{9}$$

where ω_0 = fundamental frequency of the elastic structure in the direction considered, h, G and E are defined in fig.5, N = number of stories, g = acceleration of gravity and τ = ratio of total vertical load to the inertial weight used to compute the fundamental frequency (typically around 1.1 since it is reasonable to assume a reduced live load during the extreme event).

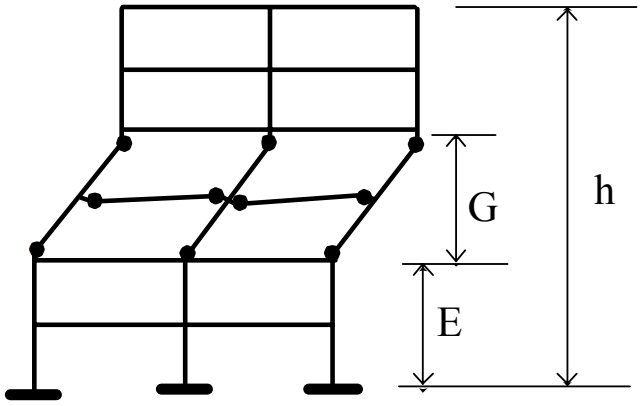

Fig.5 Parameters that define the critical mechanism

The SDOF to investigate instability has a unit mass and a damping equal to the damping of the fundamental mode, the envelope of its first order load deformation curve is assumed elasto-plastic with a yield level given by the shear V_u and the elastic stiffness is selected such that the elastic period is

$$T_e = \frac{T_1}{\sqrt{Q}} \tag{10}$$

where T_1 is the period of the fundamental mode in the structure (in the direction of analysis) and

$$Q = 1 + \theta_m - \theta_0 \tag{11}$$

The second order curve is obtained from the first order one by using the effective stability coefficient

$$\theta_e = \frac{\theta_m}{Q} \tag{12}$$

The first and second order load deformation relations (per unit mass) are illustrated in fig.6.

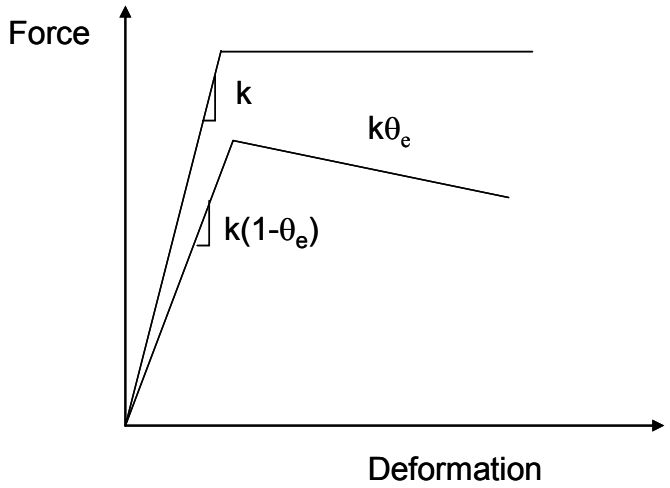

Fig.6 First and second order curves of SDOF reduction for instability analysis

A check against instability can be carried out by subjecting the SDOF reduction described previously to a set of appropriate ground motion time histories. The need to have explicit ground motions and to perform non-linear dynamic analyses, however, detracts from practicality. A much more practical approach consists in characterizing the collapse level response in terms of the relevant parameters of the SDOF reduction and the critical parameters of the ground motion using the concept of collapse spectra (Bernal 1993, 1998).

Collapse Spectra

Collapse spectra are plots vs. period (based on the initial elastic stiffness) of the minimum yield strength (per unit mass) of a SDOF for which the response is stable. These spectra can be viewed as the limit to which inelastic spectra converge when the ductility is arbitrarily large and second order effects are considered. Collapse spectra are conveniently plotted for a specific record for a constant stability coefficient. To aid clarity, the collapse spectrum for a record obtained during the Parkfield event of 2004 is depicted in Fig.7 for two values of the stability coefficient. Collapse spectra are little affected by damping so it is

customary to use 5% of critical damping based on the initial first order elastic characteristics of the SDOF system.

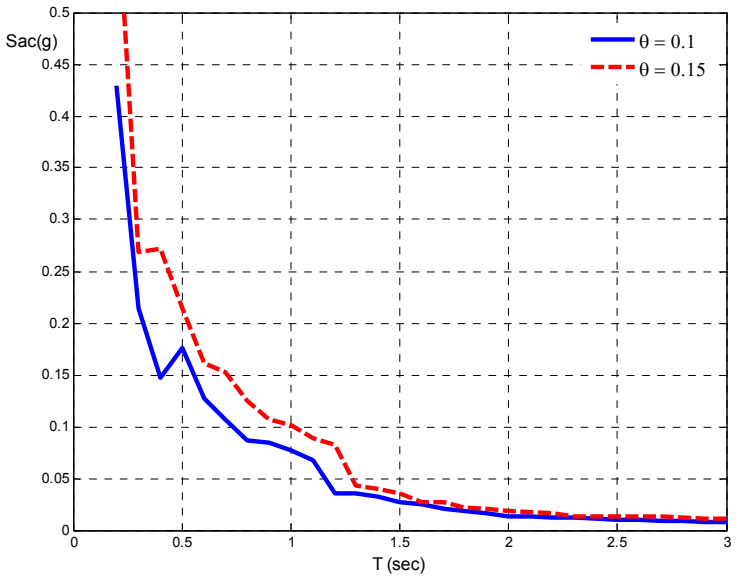

Fig.7 Collapse spectra for Parkfield 9/28/04 Vineyard Canyon 3 west station projected to the fault normal direction

Procedures to estimate elastic and inelastic spectra in terms of peak ground motion parameters and ductility (in the inelastic case) have long been available (Newmark and Hall 1982, Ridell 1979). Statistical formulas for collapse spectra were developed for systems with elasto-plastic and degrading stiffness hysteresis by Bernal (1993) using a set of far field records. At the mean level the formula for the elasto-plastic hysteresis is

$$S_{ac} = \frac{5PGV.t_{0.9}{}^{0.5}\theta^{0.75}}{T^{1.42}} \leq \frac{36PGD \cdot t_{0.9}^{0.2}\theta^{0.75}}{T^{1.86}} \tag{13}$$

where PGV and PGD stand for peak ground velocity and peak ground displacement, T is the period in sec. and $t_{0.9}$ is the effective duration of the ground motion, defined as the time over which the cumulative integral of the squared acceleration goes from 5% to 95% of its total value at the end of the record. The estimation of the minimum base shear strength for which the response is stable is taken as

$$V_c = S_{ac}M \tag{14}$$

where S_{ac} is the collapse spectral ordinate for the fundamental period and effective stability coefficient and M is the total inertial mass of the building.

Collapse Spectra for Near Fault Motions

The SDOF reduction and the concept of collapse spectra are general but extension to the near fault condition requires determining 1) if the formulas for S_{ac} developed for the far field hold for near fault motions and 2) if the uniform load distribution is adequate for predicting the collapse mechanisms that controls when the motions are impulsive.

In this research the first question was initially examined by carrying out an extensive statistical study using a collection of 43 records obtained during the M=6 Parkfield earthquake of 09/28/04. In the study the motions were first projected in the fault normal and fault parallel directions and the analysis was carried for each set separately. It was found that eqs14 and 15 predicted the collection of collapse spectra well so, on the basis of these data it did not appear that special considerations were needed for defining S_{ac} for near fault conditions. In this regard it is worth noting that while there was some difference in results between the fault parallel and the fault normal directions the differences were not sufficiently large to warrant special treatment.

Nevertheless, since the Parkfield event of 2004 is relatively low magnitude (M=6) and directivity effects in near fault motions are more prevalent in large magnitude events it was judged prudent to look at a second ensemble of near fault records before arriving at conclusions. To do this a number of records that displayed significant near fault effects were identified and the ones chosen for analysis are listed in Table 2. The motions in Table 2 were also projected in the fault normal and fault parallel orientations and the analysis was carried out independently in each direction. In contrast with the Parkfield data the analysis in this case did suggest that special expressions for predicting Sac for near fault conditions may be useful.

Table 2. Near fault records used in the study to complement the Parkfield data.

Number	Location	Date	Mw	Station	Distance (km)	Strike Angle	Angle		Rotation Angle
							Chanel 1	Chanel 2	
1	Kobe, Japan	16-Jun-95	6.9	TAZ	0.4	45	0	90	140
2	Nahanni-Canada	23-Dec-85	6.8	SITE2	5.2	160	240	330	5
3	Tabas-Iran	16-Sep-78	7.11	TAB	1.2	330	344	74	256
4	Imperial Valley,CA	15-Oct-79	6.5	E04	6	143	140	230	274
5	Imperial Valley,CA	15-Oct-79	6.5	E05	2.7	143	140	230	274
6	Imperial Valley,CA	15-Oct-79	6.5	E06	0.3	143	140	230	274
7	Imperial Valley,CA	15-Oct-79	6.5	E07	1.8	143	140	230	94
8	Imperial Valley,CA	15-Oct-79	6.5	EMO	1.2	143	270	0	324
9	Supersition Hills,CA	24-Nov-87	6.4	PTS	0.7	130	225	315	355
10	Loma Prieta CA	17-Oct-89	6.9	LGP	3	130	0	90	220
11	Loma Prieta CA	17-Oct-89	6.9	STG	8.3	130	0	90	40
12	Erzincan, Turkey	13-Mar-92	6.63	ERZ	2	125	0	90	214
13	Landers, CA	28-Jun-92	7.2	LUC	1.1	335	0	75	233
14	Northridge, CA	17-Jan-94	6.7	JFA	5.2	120	292	22	280
15	Northridge, CA	17-Jan-94	6.7	RRS	6	120	228	318	344
16	Northridge, CA	17-Jan-94	6.7	SCG	5.1	120	52	142	160
17	Northridge, CA	17-Jan-94	6.7	SCH	5	120	288	18	291
18	Northridge, CA	17-Jan-94	6.7	NWS	5.3	120	316	46	76
19	Chi Chi, Taiwan	20-Sep-99	7.6	TUC052	0.8	60	0	90	90
20	Chi Chi, Taiwan	20-Sep-99	7.6	TUC068	0.2	60	0	90	90
21	Chi Chi, Taiwan	20-Sep-99	7.6	TUC075	0.6	60	0	90	270
22	Chi Chi, Taiwan	20-Sep-99	7.6	TUC129	1.5	60	90	0	0

The statistical analysis used to arrive at the expressions for collapse spectra is summarized next.

1. Data on collapse spectra was generated from simulations.

For each of the records in Table 2, S_{ac} was computed by running nonlinear second order dynamic analysis with different strength levels until the minimum strength to prevent instability was identified. This was done for $\theta = \{0.05, 0.1, 0.15, 0.2\}$ for systems varying in period from 0.2 to 6.0 seconds.

2. The collapse spectra were normalized to $GMP \cdot t_{0.9}^{\gamma}$ where GMP was PGA, PGV or PGD and γ is a constant taken as 0, 0.1, 0.2 etc up to 1.0.

A total of 33 plots of coefficient of variation (COV) vs. period for the generated collapse spectra were obtained. For each ground motion parameter there is an exponent of the effective duration that minimizes the COV in the region where the parameter is most effective in reducing the spread. A plot of COV for the 3 optimal combinations $GMP \cdot t_{0.9}^{\gamma}$ is depicted in fig.8 for the fault normal and the fault parallel directions for $0 \leq T \leq 3$ sec. Note the level of the COV, between 0.3 and 0.4 when the appropriate normalization is selected, is typical of statistical work for the definition of spectra (Newmark and Hall 1982). Results for T> 3 sec. can be found in Ref.1.

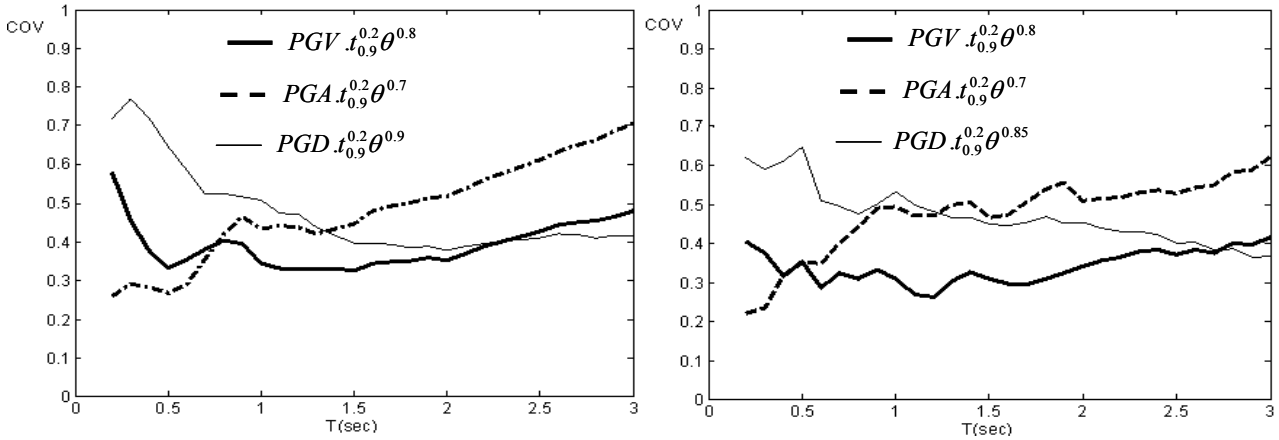

Fig. 8- COV of normalized collapse spectra to different peak ground parameter
a) fault normal component b) fault parallel component

3. The expression given in eq.15 was postulated and the free parameters $\{\alpha, \beta, \gamma, \lambda\}$ selected to minimize the spread between the predictions and the data.

$$S_{ac} = \frac{\alpha \theta^{\beta} GMP\, t_{0.9}^{\lambda}}{T^{\gamma}} \tag{15}$$

The units of S_{ac} are the same as the units in PGA or those in PGV divided by sec. or in PGD divided by sec^2. The optimum values for the free parameters are listed in Table 3.

Table 3. Optimal values of the free parameters in eq.15

GMP	Fault Normal				Fault Parallel			
	α	β	γ	λ	α	β	γ	λ
PGA	1.53	0.7	0.2	0.57	1.97	0.7	0.2	0.42
PGV	12.05	0.8	0.2	1.51	10.04	0.8	0.2	1.17
PGD	42.66	0.9	0.2	1.94	61.91	0.85	0.2	2.21

Although the coefficients in Table 3 were obtained by minimization over a fixed frequency band, in practice it is best to use the eq.15 without imposing fixed transitions because this avoids discontinuities. In particular, at any period one simply takes S_{ac} as the smallest value obtained from any of the 3 possible normalizations. A quick appreciation of the accuracy of eq.15 when compared to the simulated data can be developed from fig.9, which shows predictions and simulations at the mean level.

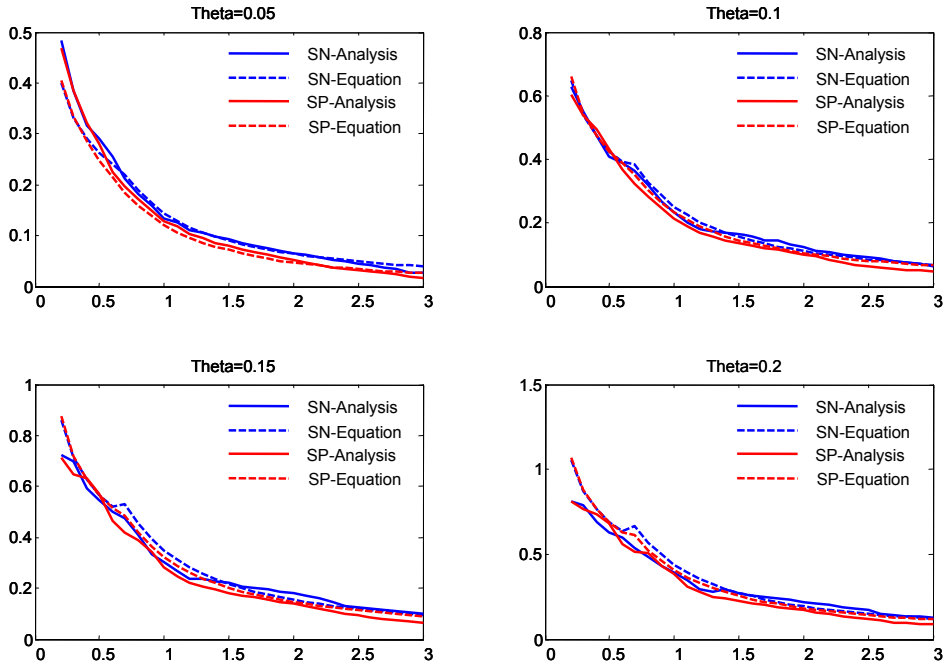

Fig.9. Comparison of actual Sac from numerical analysis with Sac from eq.15 and the coefficients in Table 3 (mean level results, in g's).

Instability Limit Reduction Factor (R_c) and the Instability Severity Index (ISI)

Before moving on to multistory buildings it is useful to pose the question: is the near fault condition critical regarding instability? The key to answering this in a meaningful way is to look

at it from a perspective that is entirely dependent on frequency content and duration. An index that satisfies the previous requirement is the ratio of the minimum strength needed to ensure that the response is elastic to the strength bellow which instability takes place. Note that this ratio is the limit that instability imposes on the classical reduction factor R which codes have long used to estimate the strength level that needs to be provided in design as a fraction of the elastic response level. We have, therefore

$$R_c = \frac{S_{ae}}{S_{ac}} \tag{16}$$

The interest lays in determining whether R_c is typically larger or smaller in the near fault than in the far field, where a large value means that instability does not pose a strong limit. For this purpose one can define an Instability Severity Index (ISI) as the inverse of the ratio of the R_c value associated with the near fault condition divided by some R_c for the far field that serves as a reference, specifically

$$ISI = \frac{1}{\frac{R_c^{\text{near fault}}}{R_c^{\text{far field}}}} \tag{17}$$

Substituting the expressions for R_c in terms of S_{ac} and S_{ae} one finds that ISI can also be written as

$$ISI = \left(\frac{S_{ae}^{\text{far field}}}{S_{ae}^{\text{near field}}} \right) \left(\frac{S_{ac}^{\text{near field}}}{S_{ac}^{\text{far field}}} \right) \tag{18}$$

In eq.18 the first ratio is always less than or equal to one because the near field effect either increases the elastic spectral ordinate or leaves it unaffected. One gathers then, that for ISI to be greater than unity (i.e., for the near fault condition to be “more severe” in the sense that we’re here characterizing it, the increase in the minimum strength to prevent collapse has to be larger than the reduction of the first term. Plainly, if the near fault condition requires x% increase in elastic strength and y% increase in the minimum strength for stability then we say that the near fault condition is severe (i.e., ISI >1) if y > x.

Fig.10 plots ISI where S_{ac} is obtained from eqs.13 and 15 for the far field and near fault condition respectively and S_{ae} is computed using the well known Newmark-Hall elastic response Spectrum construction approach with the near fault effect considered using the factors in Table.1. While fig.10 corresponds to a specific set of parameters, the qualitative behavior displayed holds for a wide range, namely: ISI is typically less than unity for short periods and for rather long periods but can exceed one in some intermediate range. Although the results show clear differences in the fault normal and fault parallel directions we refrain from making observations on this regard because the information in Table 1 is not direction specific. The fact that ISI is less than unity for long periods is consistent with what one anticipates from a qualitative reasoning since long period structures necessarily fail by crawling and the near fault motion is less capable of forcing this mechanism given the small number of significant pulses. In the short period range the reason is less intuitively evident but mathematically it derives from the

fact that the increase in the elastic spectral ordinate is larger than the increase in the strength to prevent collapse.

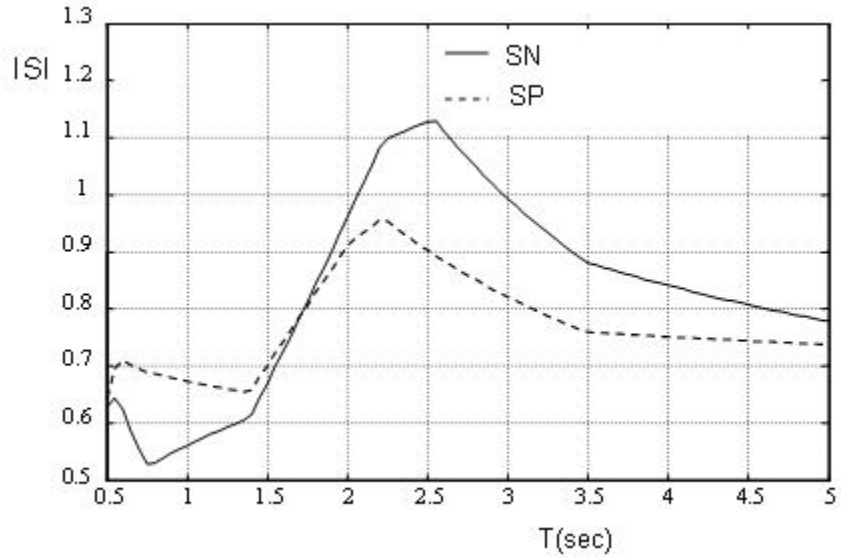

Fig.10 Instability Severity Index vs period (PGV/PGA=0.124 sec, PGD/PGV=0.48 sec $\theta = 0.1$, $t_{0.9} = 10$ sec, Na=1.2, $N_v = 1.6$ (from Table 1))

Examination of Multistory Structures

In this part of the research 3 multistory structures were considered and results computed for a large ensemble of records from the Parkfield event and for 9 motions taken from the set that appears in Table 2. The study can be subdivided into two large sections: 1) computation of ISI indices and 2) investigation of the accuracy that can be attained in predicting instability using the SDOF reduction approach described previously and the collapse spectral ordinate expression presented as eq.15 (with the coefficients in Table 3).

Mathematical Modeling

As noted earlier in the paper, the formulation of an accurate model for a 3-D structure to investigate the response up to collapse from instability is difficult. In this study a significant simplification resulted because all the structures considered are regular in plan so little is lost by using a 2D model to represent the structure. An issue that was of some concern is whether a lumped plasticity model would introduce significant error in the estimation of the collapse threshold when compared to results obtained with a distributed plasticity. The idea is that since the loss of tangent stiffness is much more gradual in the distributed plasticity model the plastic hinge simplification could prove unduly conservative. The matter was investigated by preparing two models for a 20 story structure, one where plasticity in the elements was modeled with plastic hinges and the other using fiber elements. The results showed that, at least for the type of sections used in the buildings (standard W shapes) the difference in the collapse intensity was

nominal so, for computational convenience, all models were formulated using the plastic hinge simplification. Gravity loads not acting on lateral load resisting frames were added into the models by means of an auxiliary unstable linkage that added to the geometric stiffness computation. All the buildings considered resist lateral forces through steel moment frames so the hysteretic behavior at the critical sections was assumed elasto-plastic. Moment axial force interaction was considered in the yield criterion for columns and the effect of the initial stress existing at the onset of the earthquake (due to the gravity loading) was modeled. Damping was taken to be Rayleigh type with 2% assigned to the first and second frequencies of the elastic model. As is standard, the masses were lumped at the floor levels. The boundary condition at the base, in all cases, was assumed fixed. Table 4 gives all the relevant information needed for subsequent discussion in the buildings. Sketches of the floor plans and elevations are given in Fig.11.

Table 4. Parameters of the buildings needed in the investigation of instability

Building	h (ft)	Mechanism Parameters			Period (sec)	Effective Stability Coefficient θ_e
		V_u (kips)	E	G(ft)		
6-story	82.5	902.7	0	17.5	1.58	0.119
9-story	122	2270.3	0	57	2.04	0.070
20-story	246	596.9	0	90	2.71	0.083

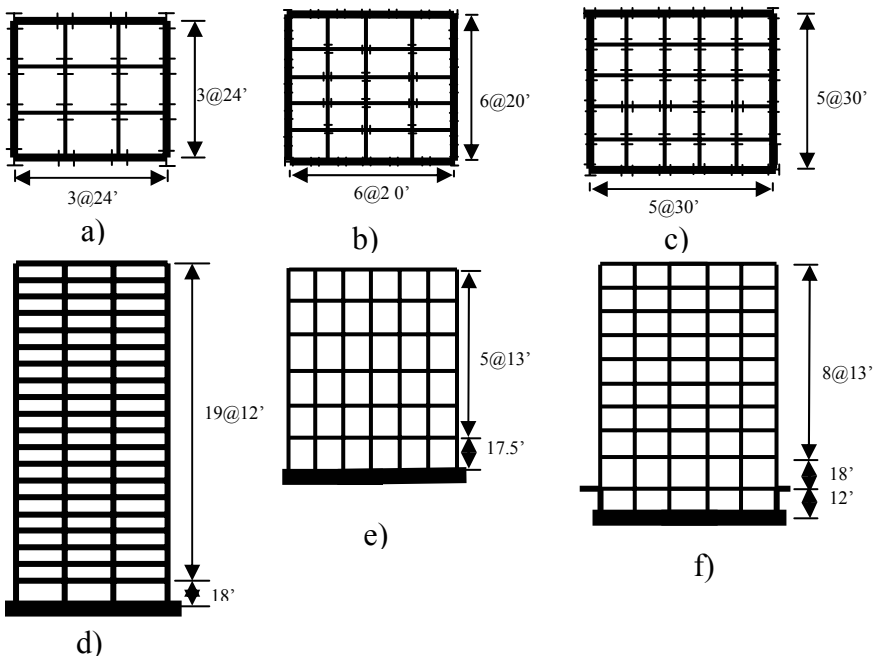

Fig.11 Floor plans and elevations of the buildings used in the multistory study

ISI Indices

The ISI index given by eq.18 can be computed for a particular near fault motion (instead of statistically) if one chooses a far field record to use as a reference. For the multistory structures we selected 10 far field records as references and computed the ISI for 23 records from Parkfield and for 9 of the records in Table 2. The results for the case of the motions from Table 2 are summarized in Table 5. The results show that the mean value of ISI is not far from unity, which is what one anticipates based on the results obtained in the SDOF analysis.

Table 5a. ISI indices for 6-story building

6-Story Building		Far Field Earthquakes									
		F1	F2	F3	F4	F5	F6	F7	F8	F9	F10
Near Field Earthquakes	N1[1]	1.15	0.78	0.71	0.80	0.86	0.80	1.44	0.87	1.15	1.64
	N2	0.91	0.62	0.56	0.63	0.68	0.63	1.14	0.69	0.91	1.30
	N3	1.50	1.03	0.93	1.04	1.12	1.04	1.88	1.13	1.51	2.15
	N4	1.69	1.16	1.05	1.17	1.27	1.18	2.12	1.28	1.70	2.42
	N9	0.66	0.45	0.41	0.46	0.50	0.46	0.83	0.50	0.67	0.95
	N10	0.86	0.59	0.53	0.60	0.65	0.60	1.08	0.65	0.87	1.23
	N12	1.36	0.93	0.84	0.94	1.02	0.95	1.70	1.03	1.37	1.95
	N14	1.39	0.95	0.87	0.97	1.05	0.97	1.75	1.05	1.40	2.00
	N19	1.03	0.71	0.64	0.72	0.77	0.72	1.29	0.78	1.04	1.48
Mean		1.17	0.80	0.73	0.81	0.88	0.82	1.47	0.89	1.18	1.68
COV		0.29	0.29	0.29	0.29	0.29	0.29	0.29	0.29	0.29	0.29

1. Refers to the # in Table 2.

Table 5b. ISI indices for 9-story building

9-Story Building		Far Field Earthquakes									
		F1	F2	F3	F4	F5	F6	F7	F8	F9	F10
Near Field Earthquakes	N1	0.60	0.29	0.16	0.44	0.35	0.27	0.43	0.35	0.36	0.37
	N2	1.35	0.66	0.36	0.99	0.78	0.62	0.97	0.78	0.81	0.84
	N3	1.59	0.78	0.43	1.17	0.92	0.73	1.14	0.92	0.95	0.99
	N4	2.33	1.15	0.62	1.72	1.35	1.07	1.67	1.35	1.40	1.46
	N9	0.62	0.31	0.17	0.46	0.36	0.29	0.45	0.36	0.37	0.39
	N10	1.71	0.84	0.46	1.26	0.99	0.78	1.22	0.99	1.02	1.07
	N12	0.88	0.43	0.24	0.65	0.51	0.41	0.63	0.51	0.53	0.55
	N14	1.68	0.83	0.45	1.24	0.97	0.77	1.20	0.97	1.00	1.05
	N19	1.14	0.56	0.31	0.84	0.66	0.53	0.82	0.66	0.69	0.72
Mean		1.32	0.65	0.35	0.98	0.77	0.61	0.95	0.77	0.79	0.83
COV		0.43	0.43	0.43	0.43	0.43	0.43	0.43	0.43	0.43	0.43

Table 5c. ISI indices for 20-story building

20-Story Building		Far Field Earthquakes									
		F1	F2	F3	F4	F5	F6	F7	F8	F9	F10
Near Field Earthquakes	N1	1.11	0.44	0.62	0.56	0.86	0.37	0.80	0.87	0.75	0.74
	N2	1.86	0.75	1.04	0.95	1.44	0.63	1.34	1.46	1.25	1.25
	N3	3.67	1.47	2.06	1.87	2.85	1.24	2.64	2.88	2.48	2.46
	N4	2.94	1.18	1.65	1.50	2.28	0.99	2.11	2.31	1.98	1.97
	N9	1.13	0.45	0.63	0.57	0.87	0.38	0.81	0.88	0.76	0.76
	N10	1.61	0.65	0.90	0.82	1.25	0.54	1.16	1.26	1.09	1.08
	N12	1.25	0.50	0.70	0.64	0.97	0.42	0.90	0.98	0.84	0.84
	N14	1.36	0.55	0.76	0.69	1.05	0.46	0.98	1.07	0.92	0.91
	N19	1.77	0.71	0.99	0.90	1.37	0.60	1.27	1.39	1.19	1.19
Mean		1.86	0.74	1.04	0.94	1.44	0.63	1.33	1.46	1.25	1.24
COV		0.48	0.48	0.48	0.48	0.48	0.48	0.48	0.48	0.48	0.48

Table 5d. Far field records used in the study

Far Field Earthquakes	F1	El centro (1940) NS
	F2	Imperial Valey 1979/09/15
	F3	Loma Prieta 1989/10/18
	F4	Kern County 1952/07/21
	F5	Big Bear 1992/06/28 08:05
	F6	Landers 1992/06/28 04:58
	F7	Northridge 1994/01/17 12:31
	F8	Petrolia 1992/05/25 11:06 PDT
	F9	Victoria , Mexico 06/09/80 03:28
	F10	Whittier Narrows 1987/10/01 14:42

Instability Predictions

The critical item from a practical perspective is whether one can estimate the collapse threshold intensity with adequate accuracy using a procedure that lends itself to practical implementation. As noted at the outset, the framework introduced by Bernal (1993, 1998) is based on reducing the multistory structure to a SDOF system that has a certain effective stability coefficient and strength and whose first order period is closely connected to that of the first mode of the building in the direction of analysis. The basic idea is that the safety margin against instability can be characterized as the ratio of the base shear strength of the mechanism to the base shear strength for which instability is imminent. The safety against instability computed in this manner can be also be interpreted as a scaling factor that if applied to the ground motion definition renders the safety margin equal to one. The adequacy of the SDOF reduction can be checked, therefore, by comparing the scaling factor that is needed to induce instability with the scaling factor predicted using the SDOF reduction. There are two ways to perform the comparison: one is by computing the collapse spectral ordinate for a given record from its definition, i.e., by performing nonlinear second order analysis and the other is by using the estimate that can be obtained from the peak ground motion parameters and the statistical expression given by eq.15. In the report presented in Ref.1 results are given for both options and

for all the Parkfield records but here we limit the presentation to the case of the motions taken from Table 2 and to the estimate of S_{ac} obtained from eq.15. The results are summarized in Table 6.

Table 6a. Summary of instability scaling factor predictions for 6-story building

6-Story Building		Fault Normal			Fault Parallel		
		Actual	Prediction	Ratio	Actual	Prediction	Ratio
Near Field Earthquakes	N1	1.50	2.19	0.68	3	1.92	1.56
	N2	8.00	4.87	1.64	5	1.92	2.61
	N3	1.20	1.05	1.14	1.2	1.46	0.82
	N4	1.50	1.77	0.85	2.7	3.37	0.80
	N9	1.40	1.45	0.96	2.5	3.09	0.81
	N10	1.30	1.36	0.95	1.7	2.13	0.80
	N12	1.90	1.58	1.21	2.2	2.88	0.76
	N14	1.05	1.26	0.83	1.3	1.53	0.85
	N19	1.03	0.79	1.30	0.9	0.99	0.91
			Mean	1.06		Mean	1.10
			COV	0.28		COV	0.56

Table 6b. Summary of instability scaling factor predictions for 9-story building

9-Story Building		Fault Normal			Fault Parallel		
		Actual	Prediction	Ratio	Actual	Prediction	Ratio
Near Field Earthquakes	N1	8.50	4.38	1.94	6.1	4.36	1.40
	N2	16.20	9.73	1.67	14	4.35	3.22
	N3	1.70	2.11	0.81	4	3.31	1.21
	N4	2.25	3.53	0.64	7.5	7.64	0.98
	N9	4.20	2.91	1.45	12	7.02	1.71
	N10	2.20	2.73	0.81	7.5	4.83	1.55
	N12	4.50	3.15	1.43	4.25	6.53	0.65
	N14	1.75	2.51	0.70	3.5	3.47	1.01
	N19	2.00	1.58	1.27	1.4	2.24	0.63
			Mean	1.19		Mean	1.37
			COV	0.39		COV	0.57

Table 6c. Summary of instability scaling factor predictions for 20-story building

20-Story Building		Fault Normal			Fault Parallel		
		Actual	Prediction	Ratio	Actual	Prediction	Ratio
Near Field Earthquakes	N1	7.00	3.98	1.76	5.25	4.37	1.20
	N2	14.10	8.83	1.60	11.5	4.36	2.64
	N3	1.40	1.91	0.73	3.5	3.32	1.05
	N4	1.75	3.21	0.55	5.25	7.66	0.69
	N9	3.75	2.64	1.42	7.5	7.04	1.07
	N10	1.90	2.48	0.77	5.5	4.84	1.14
	N12	4.75	2.86	1.66	4.5	6.54	0.69
	N14	2.20	2.28	0.96	3.3	3.48	0.95
	N19	1.50	1.43	1.05	1.3	2.24	0.58
			Mean	1.17		Mean	1.11
			COV	0.39		COV	0.55

As can be seen from the results, the predictions of the SDOF approach with the statistical expressions are conservative in the mean and provide sufficient accuracy to be useful for practical design.

Conclusions

In multistory structures subjected to strong earthquake plasticity travels along the height of the structure in a wave like fashion. Analyses show that the distribution of plastic hinges during the response can be sufficiently extensive for the effective second order stiffness to develop negative eigenvalues opening up the potential for instability. An important aspect about instability during earthquake response is the fact that its conceptualization through pseudo-static reasoning is misleading. As the paper repeatedly notes, the correct framework is not one of amplifications but of ensuring that the strength provided is sufficiently larger than that bellow which instability can be anticipated.

An indicator of how the P-delta effect interacts with the type of record is the ratio of the minimum strength needed for elastic response to the minimum strength needed to prevent instability, R_c. On the premise that design is carried out for a certain fraction of the demand computed for elastic response one concludes that the relevance of P-delta increases as R_c decreases. Results show that for large fundamental periods R_c is generally larger for near fault conditions than in the far field, indicating that being at close distances from the fault is not a critical situation for tall flexible structures from an instability perspective (provided that the elastic demand is adequately estimated). The situation can be reversed in the intermediate period range (say from 1.5 to 3 seconds) for some conditions but the reductions in R_c are typically modest and not a source for major concern. The previous observations apply both in the fault normal and fault parallel orientations although the fault normal direction is consistently the one where the effect being described is more pronounced.

Acknowledgement

The research reported in this paper was supported by the California Strong Motion Instrumentation Program (CSMIP) through Standard Agreement N0. 1004-803. This support is gratefully acknowledged.

References

Bernal D. (2006). Instability inducing potential of near-fault ground motions, CSMIP *report on data interpretation project*.

Bernal, D.(1990). P-D effects and instability in the seismic response of buildings, *Report no. CE-90-14*, Northeastern University, Boston, MA.

Bernal, D. (1991). "Dynamic instability in buildings", *Proceedings of the 6th Canadian Conference on Earthquake Engineering*, Toronto, pp. 85-92.

Bernal, D. (1992a).“Instability of buildings subjected to earthquakes”, *Journal of Structural Engineering*, ASCE, Vol. 18, No.8, pp. 2239-2260.

Bernal, D. (1992b). Dynamic instability in buildings subjected to earthquakes, *Report no. CE-92-14, Northeastern University*, Boston, MA, 1992.

Bernal, D. (1998). “Instability of buildings during seismic response”, *Engineering Structures,* vol.20, No.4-6, pp.496-502.

Bray, J.D. and Rodriguez-Marek, A. (2004) "Characterization of forward-directivity ground motions in the near-fault region". *Soil Dynamics and Earthquake Engineering,* 24, 815-828.

Husid, R. (1967). Gravity effects on the earthquake response of yielding structures, *Earthquake Engineering Research Laboratory*, California Institute of Technology, Pasadena.

Jennings P.C. and Husid, R. (1968). “Collapse of yielding structures under earthquakes”, *Journal of Engineering Mechanics*, ASCE, Vol94, No.5, pp.1045-1065.

MacRae, G.A., Morrow, D.V. and Roeder, C.W., (2001), “Near fault ground motion on simple structures”, *Journal of Structural Engineering,* ASCE, Vol.127, No.9, pp.996-1004.

Mavroeidis G.P., Dong, G. and Papageorgiou A.S., (2004). “Near-fault ground motions, and the response of elastic and inelastic single-degree-of-freedom (SDOF) systems”, *Earthquake Engineering and Structural Dynamics*, Vol.33 pp.1023-1049.

Newmark, N. M., and W. J. Hall (1982). Earthquake spectra and design, *Earthquake Engineering Research Institute*, Oakland, California.

Pique, J. (1976). On the use of simple models in nonlinear dynamic analysis, *report R76-43* Massachusetts Institute of Technology Cambridge, MA

Riddell, R. and Newmark, N.M.(1979). Statistical analysis of the response of nonlinear systems subjected to earthquakes *Res. Report R76-43*, University of Illinois, Urbana, Ill.

Somerville, P., Smith, N., Graves, R. and Abrahamson, N. (1997). “Modification of empirical strong motion attenuation relations to include the amplitude and duration effects of rupture directivity” *Seismological Res. Letters,* 68(1), 199-222.

Takizawa, H. and Jennings, P. (1980). “Collapse of a model for ductile reinforced concrete frames under extreme earthquake motions”, *Earthquake Engineering and Structural Dynamics,* Vol.8, pp.117-144.